Published OnlineFirst March 27, 2013; DOI: 10.1158/0008-5472.CAN-12-3970

Cancer Research

Interleukin-1β Promotes Skeletal Colonization and Progression of Metastatic Prostate Cancer Cells with Neuroendocrine Features

Qingxin Liu[1], Mike R. Russell, Kristina Shahriari[1], Danielle L. Jernigan[1], Mercedes I. Lioni[2], Fernando U. Garcia[2], and Alessandro Fatatis[1,2,3]

Abstract

Despite the progress made in the early detection and treatment of prostate adenocarcinoma, the metastatic lesions from this tumor are incurable. We used genome-wide expression analysis of human prostate cancer cells with different metastatic behavior in animal models to reveal that bone-tropic phenotypes upregulate three genes encoding for the cytokine interleukin-1β (IL-1β), the chemokine CXCL6 (GCP-2), and the protease inhibitor elafin (PI3). The Oncomine database revealed that these three genes are significantly upregulated in human prostate cancer versus normal tissue and correlate with Gleason scores ≥7. This correlation was further validated for IL-1β by immunodetection in prostate tissue arrays. Our study also shows that the exogenous overexpression of IL-1β in nonmetastatic cancer cells promotes their growth into large skeletal lesions in mice, whereas its knockdown significantly impairs the bone progression of highly metastatic cells. In addition, IL-1β secreted by metastatic cells induced the overexpression of COX-2 (PTGS2) in human bone mesenchymal cells treated with conditioned media from bone metastatic prostate cancer cells. Finally, we inspected human tissue specimens from skeletal metastases and detected prostate cancer cells positive for both IL-1β and synaptophysin while concurrently lacking prostate-specific antigen (PSA, KLK3) expression. Collectively, these findings indicate that IL-1β supports the skeletal colonization and metastatic progression of prostate cancer cells with an acquired neuroendocrine phenotype. *Cancer Res; 73(11); 1–9. ©2013 AACR.*

Introduction

The therapeutic management of patients with prostate cancer includes the blockade of androgen receptor (AR) activation and signaling based on androgen-deprivation therapy (ADT; refs. 1, 2) and receptor antagonists (3). This approach is initially remarkably effective but eventually leads to the conversion of the disease to castration-resistant prostate cancer (CRPC). The conversion to CRPC is attributed to the expression of splice variants of the AR and recruitment of alternative signaling pathways that the receptor uses to promote the growth and survival of malignant cells while escaping the effects of a range of inhibitory drugs and hormonal therapies (4, 5). Notably, ADT frequently induces the secondary emergence of highly aggressive prostate phenotypes with neuroendocrine features, including the expression of markers such as chromogranin A and synaptophysin and suppression of PSA (6, 7). Thus, while neuroendocrine prostate cancer (NEPC) is considered an aggressive subtype of the primary tumor (8), prostate disseminated tumor cells (DTC) could acquire NEPC features following ADT and during the most common clinical manifestation of the prostate cancer. As NEPC cells are independent of androgens for their growth, ADT might provide them with a selective survival advantage (9). In fact, the percentage of neuroendocrine cells sharply increases in high-grade and advanced stage prostate tumors upon establishment of ADT (10, 11). More importantly, cancer cells lacking AR and/or PSA expression are frequently detected in bone metastatic lesions among AR+ and PSA+ malignant phenotypes (12). These DTCs with acquired NEPC phenotypes could be very effective in colonizing the bone during the initial stages of metastasis and be responsible for establishing a metastatic niche that would subsequently also support the growth of AR+/PSA+ cancer cells.

Bone-metastatic disease is often fatal for patients with prostate cancer and its treatment remains an unmet medical need. The molecular underpinning for the establishment and progression of secondary bone lesions has been only partially elucidated. A better understanding of the factors regulating bone colonization, particularly the autocrine and paracrine

Authors' Affiliations: [1]Department of Pharmacology and Physiology, [2]Pathology and Laboratory Medicine, Drexel University College of Medicine; and [3]Kimmel Cancer Center, Philadelphia, Pennsylvania

Note: Supplementary data for this article are available at Cancer Research Online (http://cancerres.aacrjournals.org/).

Current address for M. Russell:, Division of Oncology, Children Hospital of Philadelphia, Colket Translational Research Building, Room 8211, 3501 Civic Center Boulevard, Philadelphia, PA 19104.

Corresponding Author: Alessandro Fatatis, Pharmacology and Physiology, 245 N. 15th Street, New College Building, Philadelphia, PA 19102. Phone: 215-762-8534; Fax: 215-762-2299

doi: 10.1158/0008-5472.CAN-12-3970

Published OnlineFirst March 27, 2013; DOI: 10.1158/0008-5472.CAN-12-3970

interactions of DTCs with the surrounding stroma, will help to find more effective therapies for the management of metastatic patients. We previously reported that the ability of prostate cancer cells to generate skeletal tumors in animal models correlates with the expression of the platelet-derived growth factor receptor alpha isoform (PDGFRα; refs. 13–15). Here, we show that PDGFRα upregulates the expression of 3 genes that were associated with the occurrence of skeletal metastases in animal models inoculated in the arterial blood circulation with human prostate cancer cells. Among these genes, interleukin (IL)-1β is independently accountable for dictating bone-metastatic behavior and was also detected in human specimens of both primary prostate cancer and bone-metastatic lesions. Finally, the coexpression of IL-1β with the NEPC marker synaptophysin in prostate cells detected in human skeletal lesions corroborates the idea that this cytokine plays a role in the progression of bone-metastatic tumors affecting patients with prostate cancer treated with ADT.

Materials and Methods

Cell lines and cell culture

NIH-3T3 and DU-145 cells were obtained from American Type Culture Collection (ATCC) and passaged in our laboratory for less than than 6 months after resuscitation. PC3-N and PC3-ML sublines were derived from the parental PC-3 cell line as previously described (16). Both sublines were tested by Idexx Radil on May 2012 by short tandem repeat-based DNA fingerprinting and confirmed to be of human origin without mammalian interspecies contamination. The alleles for 9 different markers were determined and the genetic profiles of both PC3-ML and PC3-N cells were found identical to the profiles reported for the parental PC3 line deposited with the ATCC. All prostate cancer cells lines were cultured at 37°C and 5% CO_2 in Dulbecco's Modified Eagle Medium (DMEM; Invitrogen) supplemented with 10% FBS (Hyclone) and 0.1% gentamicin (Invitrogen). We cultured all prostate cancer cell lines used in this study for 10 passages and then thawed a new frozen stock to avoid the emergence of genotypic and phenotypic changes (17). Cells were genetically engineered to stably express EGFP using a lentiviral vector (AmeriPharma). Bone marrow-derived human mesenchymal stem cells (MSC; Lonza) were used between passage 5 and 8 and cultured in MSC growth medium [α-MEM (Invitrogen) supplemented with 10% FBS, 1 ng/mL basic fibroblast growth factor (R&D Systems), and 0.1% gentamicin].

SDS-PAGE and Western blotting

Cell lysates were obtained and SDS-PAGE and Western Blot analysis conducted as previously described (18) with few modifications. Membranes were blotted with antibodies targeting IL-1β (SC-7884, Santa Cruz), actin (A-2066, Sigma-Aldrich), COX-2 (ab15191, Abcam), elafin (SC-20637, Santa Cruz), and GAPDH (D16H11, Cell Signaling Technology). Primary antibody binding was detected using a horseradish peroxidase-conjugated secondary antibody (Pierce; Thermo Scientific). Chemiluminescent signals were obtained using SuperSignal West Femto reagents (Pierce) and detected with the Fluorochem 8900 imaging system and related software (Alpha Innotech, ProteinSimple).

Conditioned media experiments

Conditioned media were obtained according to ref. 19. In brief, 7.5×10^5 PC3-ML cells were plated in 15 mL of DMEM supplemented with 10% FBS and 0.1% gentamycin and cultured for 5 days. The medium from each dish was then collected and centrifuged at 2,000 rpm for 10 minutes and then used fresh as described below.

For bone cell treatment experiments, MSCs were plated at least 48 hours before treatment; when 70% confluent, cells were incubated in a 1:1 mixture of conditioned medium and MSC growth medium for 48 hours. To pharmacologically induce the overexpression of COX-2 in MSCs, cells were exposed to 0.1 ng/mL of IL-1β (R&D Systems). Cells were preincubated with the IL-1R inhibitor Anakinra (Amgen) at a 10 μg/mL concentration for 30 minutes before being exposed to IL-1β.

ELISA measurements

The concentrations of IL-1β and CXCL6 were measured by ELISA following the manufacturers' protocols. In brief, same numbers of cells (5×10^5) were plated in 35 mm culture dishes; the next day, the medium was replaced with 1 mL of DMEM supplemented with 10% FBS and 0.1% gentamycin and cultured for 24 hours. The supernatants were then collected, the adherent cells in each dish measured again, and IL-1β or CXCL6 protein concentrations measured using Quantikine kits (R&D Systems). The ELISA data were normalized to the number of cells counted in each dish when the supernatants were collected.

Viral vectors and cell transduction procedures

Depletion of IL-1β in PC3-ML cells. Virus containing Mission TRC lentiviral vectors shRNA (Sigma-Aldrich) with sequence 5′-CGGCCAGGATATAACTGACTT-3′ were used to knockdown IL-1β expression. Subconfluent cell cultures were infected overnight in the presence of 8 μg/mL polybrene (Millipore). The successfully infected cells were selected for the ability to proliferate in media containing 600 μg/mL of G418 (Invitrogen) and protein expression was validated by Western blot analysis using an antibody against IL-1β. Cells transduced with a TRC lentiviral vector carrying a noncoding short-hairpin RNA (shRNA) were used in control experiments.

Overexpression of IL-1β in PC3-N and DU-145 cells. To prepare the IL-1β–overexpressing retrovirus, a mixture of pLXSN vector containing 50 ng of IL-1β plasmid and 8 μL of Lipofectamine 2000 (Invitrogen) was incubated at room temperature for 30 minutes. The transfection mix was transferred to phoenix cells that were approximately 70% confluent. After 16 hours, the transfection medium was replaced with growth medium containing 10% serum and the virus was harvested at 38 hours after transfection. The virus-containing medium was pooled, centrifuged at 44,000 rpm for 20 minutes, and the supernatant was used to infect PC3-N and DU-145 cells. Cells were selected for the ability to proliferate in media containing G418 (0.6 mg/mL) and the infection was further validated by Western blot analysis using an antibody against IL-1β. Cells transduced with an empty pLXSN vector were used in control experiments.

Published OnlineFirst March 27, 2013; DOI: 10.1158/0008-5472.CAN-12-3970

Animal model of metastasis

Five-week-old male immunocompromised mice (CB17-SCRF) were obtained from Taconic and housed in a germ-free barrier. At 6 weeks of age, animals were anesthetized with 100 mg/kg ketamine and 20 mg/kg xylazine administered by intraperitoneal route and successively inoculated in the left cardiac ventricle with cancer cells [5×10^4 in 100 μL of serum-free DMEM/F12 (Invitrogen)]. Cell inoculation was conducted using a 30-gauge needle connected to a 1 mL syringe. The delivery of the cell suspension in the systemic blood circulation was validated by the coinjection of blue fluorescent 10 μm polystyrene beads (Invitrogen-Molecular Probes). Animals were randomly assigned to different experimental groups and sacrificed at specified time-points following inoculation. Organs were harvested and prepared as described below and tissue sections inspected blindly for metastatic lesions. The homogeneous and numerically consistent distribution of the beads in adrenal glands and lungs collected at necropsy and inspected by fluorescence microscopy were used as discrimination criteria for the inclusion of animals in the studies.

All experiments were conducted in accordance with NIH guidelines for the humane use of animals. All animal protocols were approved by the Drexel University College of Medicine Institutional Animal Care and Use Committee (Philadelphia, PA).

Tissue processing. Bones and soft-tissue organs were collected and fixed in 4% paraformaldehyde solution (Electron Microscopy Sciences) for 24 hours and then transferred into fresh formaldehyde for an additional 24 hours. Soft tissues were then placed either in 30% sucrose for cryoprotection or 1% paraformaldehyde for long-term storage. Bones were decalcified in 0.5M EDTA (Fisher Scientific) for 7 days followed by incubation in 30% sucrose. Tissues were maintained at 4°C for all aforementioned steps and frozen in optimum cutting temperature medium (Sakura Finetek) by placement over dry-ice chilled 2-methylbutane. Serial sections of 80 μm thickness were obtained using a Microm HM550 cryostat. Femur and tibia in each knee joint were cut entirely through, resulting in approximately 30 sections per specimen made available for analysis.

Fluorescence microscopy and morphometric analysis of metastases. Fluorescent images of skeletal metastases were acquired using a Zeiss AX70 microscope (Carl Zeiss) connected to a Nuance Multispectral Imaging System. Digital images were analyzed and processed with the Nuance Software (v. 2.4). Microscope and software calibration for size measurement was conducted using a TS-M2 stage micrometer (Oplenic Optronics).

Microarray processing, normalization, and analysis

Total RNA was purified with Qiagen RNeasy Mini Kit (Qiagen). RNA quality control for each set of samples was conducted using a BioAnalyzer (Agilent). Two rounds of amplification were used according to the Affymetrix Two-cycle Amplification protocol using 25 ng for total RNA. Aliquots of 15 μg of amplified biotinylated RNA were hybridized to 1.0 Human Gene ST arrays (Affymetrix). Arrays were scanned using the GeneChip Scanner 3000 (Affymetrix). The Robust Multichip Analysis (RMA) algorithm was applied to all array data (20). GeneSpring software version 11.5 was used to filter and complete the statistical analysis. To analyze the microarray data, CEL files were loaded to GeneSpring, and probeset summarization was conducted using the RMA 16 algorithm. For each probe, the median of the log-summarized values from all the samples was calculated and subtracted from each sample. After processing and normalization, the resulting 28,869 genes included in the 1.0 Human Gene ST arrays were filtered to remove very low or saturated signal values. Each entity was filtered on raw data by percentile with an upper cutoff of 100 and a lower cutoff 20. The resulting new entities were then subjected to statistical analysis using an unpaired *t* test with a *P* value fixed at 0.05. Finally, a higher stringency filter was applied to the resulting entities using a 2.0 fold-change cutoff and the Benjamin–Hochberg multiple testing corrections. The microarray data were submitted to the gene expression omnibus (GEO) data repository and can be accessed with the number GSE43332.

Oncomine analysis

The oncomine database (available online) was searched for *IL-1β*, *CXCL6*, and *PI3* genes. The datasets containing expression data for each gene were filtered to display upregulation in prostate cancer versus normal prostate tissue with $P < 0.05$. If more than one dataset passed the filters, we conducted a meta-analysis to obtain a *P* value.

Clinical samples, immunohistochemistry, and analysis

Commercially available human tissue microarrays (TMA; PR956, PR8010, PR483, PR751) contained 192 prostate tissue cores and were obtained from US Biomax. Two additional existing TMAs containing 35 deidentified human prostate cancer specimens as well as 7 deidentified bone tissue specimens with metastatic prostate cancer were obtained from the archives of the Department of Pathology at Drexel University College of Medicine.

Immunohistochemical detection was conducted using antibodies against IL-1β (ab2105, AbCam), PSA (ER-PR8, Cell Marque), and Synaptophysin (SP11, Ventana) all diluted 1:50 on formalin-fixed paraffin-embedded sections. The staining conditions using the BenchMark ULTRA IHC/ISH Staining module were as follows: antigen retrieval (pH 8.1) using CC1 reagent 64 minutes, followed by primary antibody incubation for 40 minutes at 37°C, and then staining with the XT, Ultraview Universal DAB Detection Kit. Interpretation and scoring was conducted by 2 clinical pathologists (F.U. Garcia and M.I. Lioni) using light microscopy. Staining intensities were scored as follows 0, no staining; 1, weak staining; 2, moderate staining; and 3, strong staining. Only samples that showed 40% or more of cellular staining were used for the analysis.

Statistics

We analyzed number and size of skeletal metastases between 2 experimental groups using a 2-tailed Student *t* test and between multiple groups using a one-way ANOVA test. A value of $P \leq 0.05$ was deemed significant. The results of TMA staining were subjected to χ^2 analysis and plotted in a contingency table.

Published OnlineFirst March 27, 2013; DOI: 10.1158/0008-5472.CAN-12-3970

Results and Discussion

We conducted genome-wide comparative transcriptome analyses of human prostate cancer cell lines that differ in PDGFRα expression and propensity to establish tumors in the skeleton of animal models. First, we examined genes that were differentially regulated in the highly bone-metastatic PC3-ML cells and their low-metastatic counterpart PC3-N cells (16). Both sublines were derived from the PC3 parental cell line, which was originally obtained from a skeletal lesion in a patient with grade 4 metastatic prostate adenocarcinoma treated with ADT (21). These cells lack AR and PSA and their androgen-independent status is associated with the expression of neuroendocrine markers (22). We have previously reported that PC3-ML cells directly inoculated into the arterial circulation of severe combined immunodeficient (SCID) mice generate large skeletal lesions in more than 90% of animals (Supplementary Fig. S1A and S1C; ref. 14). These cells express high levels of PDGFRα, in contrast to PC3-N cells, which show low metastatic potential in the same animal model and express significantly lower levels of the PDGFRα (13). Microarray data analysis revealed that 16 genes were differentially expressed between high-metastatic PC3-ML and low-metastatic PC3-N cells (Supplementary Fig. S2A). Because we previously found that the overexpression of PDGFRα in PC3-N cells induces a bone-metastatic behavior identical to that of PC3-ML cells (14, 23), we investigated the genes differentially regulated between PC3-N and PC3-N(Rα) (Supplementary Fig. S2B). This approach identified 7 genes that were similarly upregulated in highly metastatic PC3-ML and PC3-N(Rα) cells as compared with low metastatic PC3-N cells (Supplementary Fig. S2C and S2D). These results were significantly strengthened by the analysis of DU-145 cells, which were isolated from a brain rather than a skeletal metastatic lesion in a patient with prostate cancer (24, 25). We have previously shown that DU-145 cells lack PDGFRα (13) and fail to survive longer than 3 days as DTCs after homing to the mouse bone marrow (Supplementary Fig. S1A and S1B; ref. 14). Interestingly, and in contrast to PC3-N cells, the exogenous expression of PDGFRα did not promote metastatic bone-tropism of DU-145 cells in our model (data not shown). Consistent with this observation, PDGFRα expression in DU-145 cells upregulated 5 genes that did not overlap with the 7 putative prometastatic genes identified in PC3 cells (Supplementary Fig. S3), suggesting their lack of involvement in the bone-metastatic behavior of prostate cancer cells. To refine these findings and compensate for the inherent genetic disparity of PC3 and DU-145 cells, we isolated 2 single-cell progenies from PC3-ML cells. When tested in our animal model, both PC3-ML clone 1 and clone 3 were highly bone-metastatic (Supplementary Fig. S4). A comparative analysis of the genes differentially regulated between these 2 clonal cell lines and our newly identified 7 gene set resulted in a final cohort of 3 upregulated genes: the inflammatory cytokine IL-1β, the chemokine CXCL6, and the leukocyte protease inhibitor elafin. These 3 genes consistently correlated with both PDGFRα expression and aggressive bone-metastatic behavior in our model. Proteomic approaches validated the transcriptome analysis and confirmed the data relative to IL-1β (Supplementary Fig. S5) as well as CXCL6 and elafin (Supplementary Fig. S6). These results were corroborated by mining prostate cancer datasets publically available through the Oncomine repository, showing that IL-1β, CXCL6, and elafin are significantly upregulated in tumors as compared with normal prostate tissues (Table 1, top). Furthermore, a

Table 1. The Oncomine database shows a consistent increase in the expression of these 3 genes in tumor as compared with normal prostate tissue (top); a significant correlation between IL-1β and CXCL6 expression in tumors with Gleason scores (7–9) and (8–9), respectively

Oncomine analysis

Analysis type: Prostate cancer versus normal

Gene	*P*	Fold PC/N	PC, *n*	N, *n*	Dataset
IL-1β	0.01	1.18	156	29	ref. 51
	0.01	1.42	13	6	ref. 52
	0.02	1.08	89	23	ref. 53
CXCL6	0.003	1.132	89	23	ref. 53
	0.022	1.269	52	50	ref. 54
Elafin (PI3)	0.008	1.131	52	50	ref. 54

Meta-analysis

Gene	Median rank	*P*
IL-1β	2239	0.029
CXCL6	1656	0.013
Elafin	Only one study	

Association with Gleason Score

Gleason score	Genes	*P*
7–9	IL-1β	0.023
8–9	CXCL6	0.013
8–9	Elafin	0.008

NOTE: Only one study analyzing Elafin expression in tumor versus normal and Gleason scores (8–9) was available (bottom).

Published OnlineFirst March 27, 2013; DOI: 10.1158/0008-5472.CAN-12-3970

meta-analysis indicated a strong association of both IL-1β and CXCL6 with prostate cancer with Gleason scores (≥7; Table 1, bottom). In light of these observations, we screened human tissue arrays including 227 cases of prostate adenocarcinoma for IL-1β protein expression and correlated signal intensities with the Gleason score attributed to each tissue specimen (Fig. 1). This approach validated the results from the Oncomine analysis and conclusively shows that prostate tumors with intermediate and high Gleason scores, which have the highest propensity to metastasize (26, 27), express increased levels of IL-1β as compared with tumors with Gleason scores (<7) or normal tissues (Supplementary Table S1). Remarkably, IL-1β inhibits the expression of both PSA (28) and AR (29) in prostate cancer cells, thus reproducing features observed in PC3-ML cells as well as NEPC cells either primarily or as a consequence of ADT (7, 30). Therefore, we reasoned that IL-1β could be a crucial player in the establishment of skeletal secondary lesions by prostate cancer. To challenge this hypothesis, we used a preclinical animal model of metastasis and used shRNA to deplete IL-1β in PC3-ML cells to levels of expression and secretion comparable with those observed in PC3-N cells (Fig. 2A and B). The resulting PC3-ML(sh-IL-1β) cells were delivered in the systemic arterial circulation of mice euthanized 4 weeks later and showed significantly impaired metastatic abilities. The inspection of femora and tibiae of inoculated animals showed that PC3-ML and PC3-ML(sh-IL-1β) cells produced bone metastases in a comparable number of animals (Fig. 2C). However, the lesions generated by PC3-ML(sh-IL-1β) cells were 70% smaller than those observed in mice inoculated with PC3-ML cells expressing endogenous levels of IL-1β. (Fig. 2D and E). It is plausible that silencing IL-1β in combination with one or both of the other 2 genes identified in this study provides superior inhibition of metastatic progression than silencing IL-1β alone. Our laboratory is currently actively pursuing the preclinical validation of this paradigm.

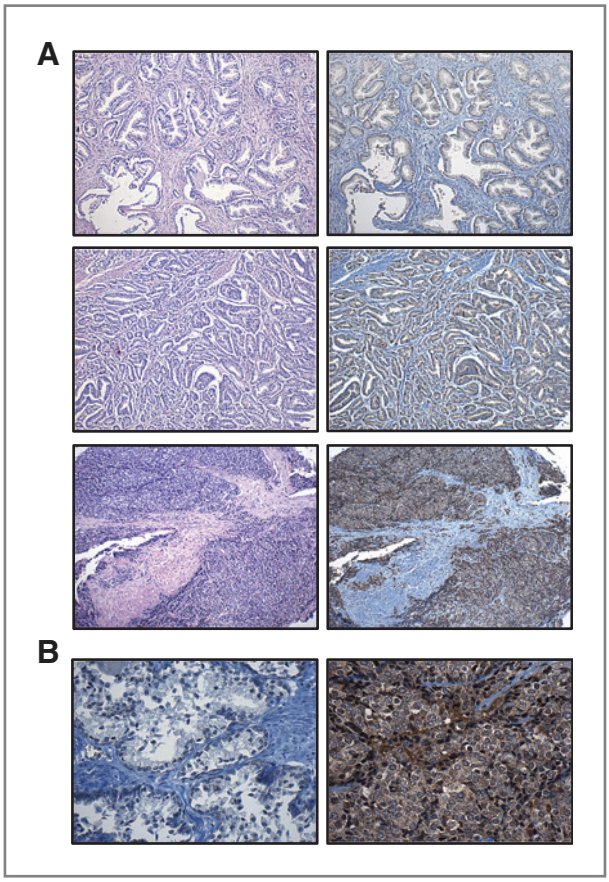

Figure 1. Upregulation of the genes for IL-1β, CXCL6, and elafin in prostate cancer. A, TMAs including 227 cases of primary prostate adenocarcinoma were stained for IL-1β with signal intensities that were scored as weak (1+, top), moderate (2+, middle), and strong (3+, bottom). B, higher magnification of 2 representative tissue specimens that stained negative (left) and strongly positive (right) for IL-1β, respectively. Hematoxylin–eosin counterstaining was used (B).

To further define the role of IL-1β in skeletal metastasis, we conducted complementary experiments in which this cytokine was exogenously overexpressed in prostate cancer cells with demonstrated inability to progress to macroscopic bone lesions. We first studied PC3-N cells, which routinely produce small lesions in only 20% of animals inspected at 3 weeks after inoculation and regress thereafter (Supplementary Fig. S1) and (14). After homing to the skeleton from the blood circulation, PC3-N(IL-1β) cells were able to fully progress into tumors comparable in number and size to the lesions produced by PC3-N(Rα) cells (Fig. 3; refs. 14, 15). More importantly, analogous results were obtained with DU-145 cells, which are widely reported to lack bone-tropism in mouse models (31). We have previously shown that this lack of metastatic behavior is caused by the inability of these cells to survive for more than 3 days after homing to the bone marrow (14). DU-145 cells do not endogenously express IL-1β (28,32); interestingly, upon overexpression of this cytokine (Fig. 4A and B) these cells generated skeletal metastases in 40% of mice examined at 4 weeks after inoculation (Fig. 4C). Although these lesions were smaller in size than the skeletal tumors produced by PC3-N(IL-1β) cells after the same time interval (Fig. 4D and E), these data provide compelling evidence that, in addition to potentiating the weak bone-tropism of PC3-N cells, IL-1β can induce *de novo* metastatic behavior in prostate cancer cells. Furthermore, the increase in tumor area observed for DU-145 (IL-1β) lesions detected 4 weeks compared with those at 2 weeks after inoculation (Fig. 4D) clearly indicates that IL-1β promotes both survival and proliferation of metastatic cells in the skeleton.

Despite originating from different metastatic sites in patients with prostate cancer, PC3 and DU-145 cells both express neuroendocrine markers (33). The acquisition of a neuroendocrine phenotype is frequently induced by the ADT commonly used for patients with advanced prostate adenocarcinoma (9, 34, 35) and is also observed in transgenic animal models of prostate cancer upon castration (36). These observations would suggest that the convergence of ADT-induced neuroendocrine transdifferentiation and increased expression of IL-1β underpins the propensity of prostate cancer cells to colonize the skeleton and eventually progress to secondary bone lesions. To test this model, we used an *ex vivo* analysis of skeletal lesions obtained from patients with

Published OnlineFirst March 27, 2013; DOI: 10.1158/0008-5472.CAN-12-3970

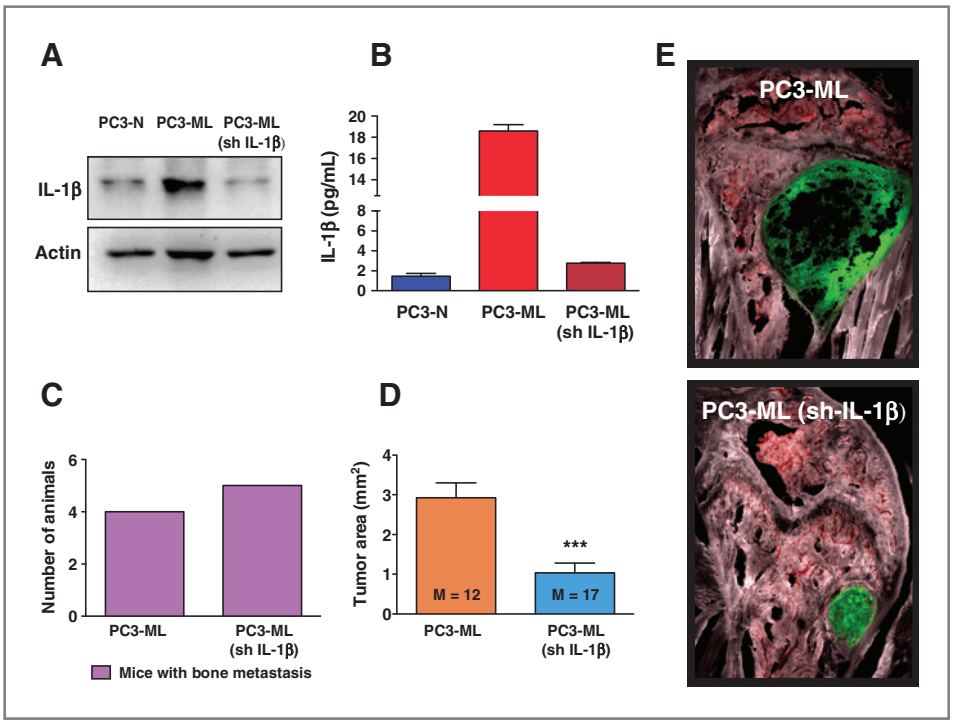

Figure 2. Effects of IL-1β silencing on the metastatic potential of prostate cancer cells *in vivo*. In highly metastatic PC3-ML cells, RNA interference reduced both the protein expression of IL-1β precursor (A) and secretion of the mature form as measured by ELISA (B); 4 weeks after intracardiac inoculation of PC3-ML or PC3-ML(sh-IL-1β) cells, all mice had developed bone metastatic tumors (C and D); however, the lesions generated by PC3-ML (sh-IL-1β) cells were significantly smaller in size (E). PC3-ML cells transduced with a TRC lentiviral vector carrying a noncoding shRNA were used in control experiments in which 5 mice were euthanized 4 weeks after inoculation and showed number and distribution of metastatic tumors comparable with parental PC3-ML cells (not shown). M, number of metastatic tumors; ***, $P = 0.002$.

advanced prostate cancer and found that all specimens stained positively for IL-1β. Interestingly, the intensity of the signal showed an inverse correlation with PSA expression (Fig. 5A), and two specimens also stained positively for synaptophysin (Fig. 5B). These results provide strong support for a role of IL-1β overexpression in bone-metastatic growth of prostate cancer cells and suggest a frequent association of this cytokine with evident NEPC features of skeletal metastases from prostate adenocarcinoma.

The secondary tropism of metastatic tumors is the result of compatibility between DTCs and the tissue microenvironment of the colonized organs (37, 38). Because of the stimulatory effect exerted by IL-1β on the bone-resorption activity of osteoclasts (39), a plausible scenario would

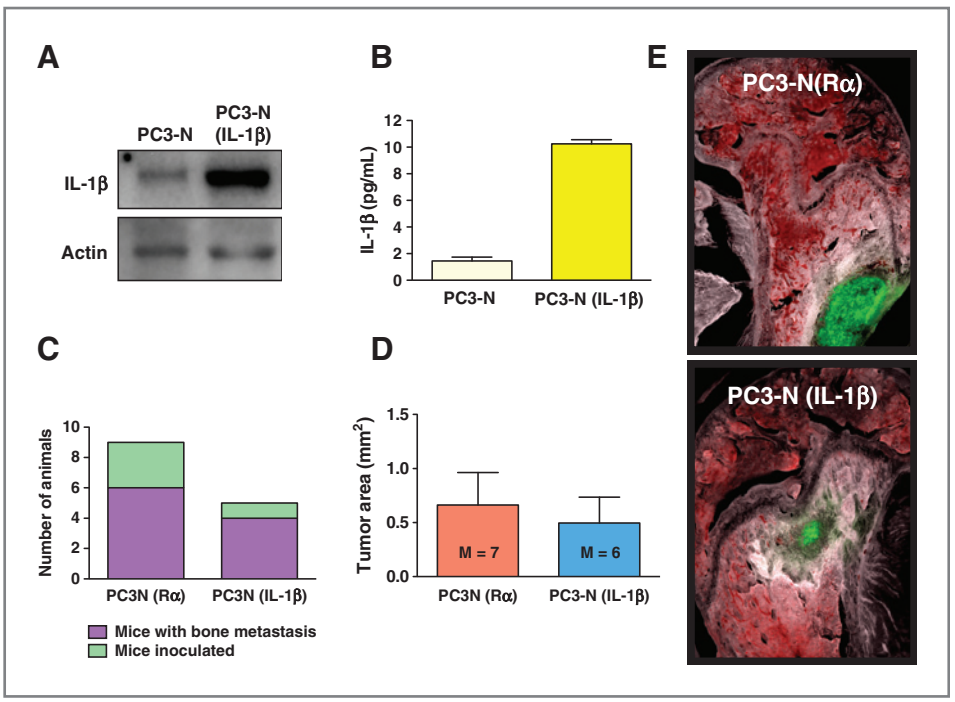

Figure 3. Effects of IL-1β overexpression on the metastatic potential of prostate cancer cells *in vivo*. IL-1β protein expression (A) and secretion (B) were exogenously increased in low-metastatic PC3-N cells; the resulting PC3-N(IL-1β) cells were as effective as PC3-N(Rα) cells in generating skeletal lesions in mice sacrificed 4 weeks after intracardiac inoculation (C) and produced bone lesions that were comparable in size (D and E). PC3-N cells transduced with an empty pLXSN vector were inoculated in the arterial circulation of 5 mice that were euthanized 4 weeks later and found to be free of skeletal tumors (not shown). M, number of metastatic tumors.

Published OnlineFirst March 27, 2013; DOI: 10.1158/0008-5472.CAN-12-3970

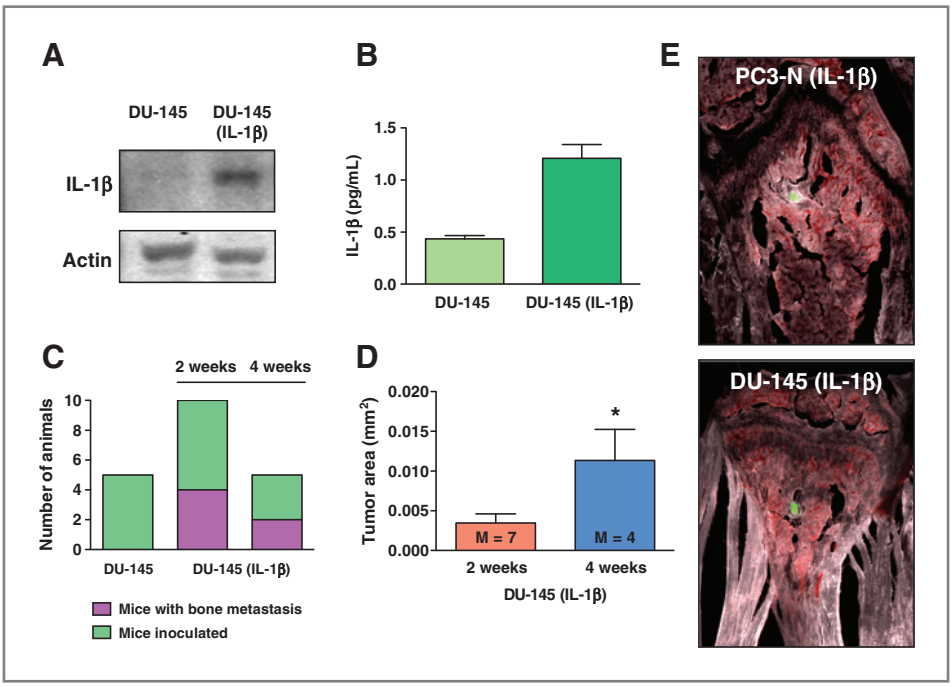

Figure 4. Exogenous expression of IL-1β in nonmetastatic DU-145 cells induces a bone-metastatic phenotype. The expression (A) and secretion (B) of IL-1β were exogenously induced in DU-145 cells, which are normally negative for this protein and nonmetastatic. C, the resulting DU-145 (IL-1β) cells generated bone lesions in 40% of mice inoculated via the intracardiac route and sacrificed either 2 or 4 weeks after inoculation. D, the size of skeletal lesions increased in a time-dependent manner, thus suggesting metastatic progression E, size comparison of bone tumors detected at 2 weeks after inoculation in mice that received PC3-N(IL-1β) or DU-145 (IL-1β) cells. M, number of metastatic tumors; *, $P = 0.037$.

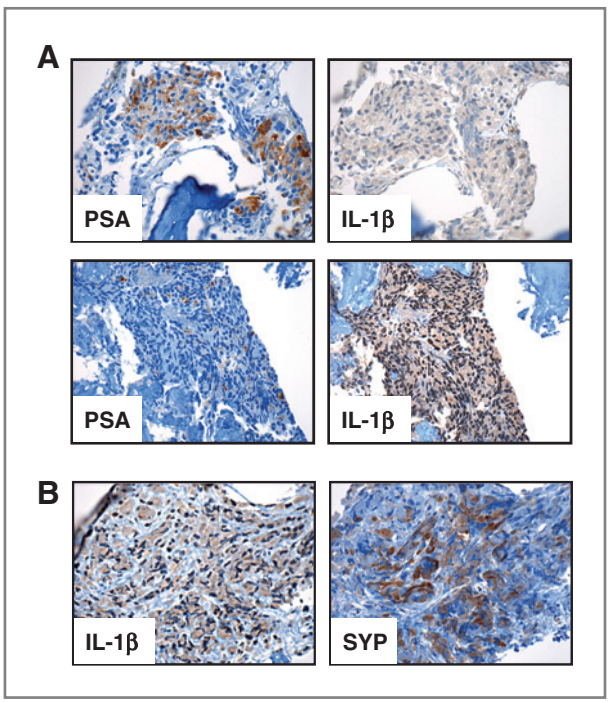

Figure 5. Detection of IL-1β protein in skeletal metastases and correlation with PSA and synaptophysin expression. Seven specimens collected from different patients with prostate cancer were analyzed. All specimens stained positive for IL-1β and the intensity of the signal seemed to be inversely correlated with the expression levels of PSA in the same areas. Representative images from 2 different tumor regions in a single patient are shown in A. Two out of 7 specimens stained positive for both IL-1β and synaptophysin (SYP; B). Magnification, ×100 for A; ×200 for B.

include this cytokine supporting secondary skeletal lesions by promoting bone matrix turnover and increasing the availability of trophic factors for the disseminated cancer cells. Indeed, this mechanism is commonly targeted by bisphosphonates and RANKL inhibitors in the clinical management of patients with metastatic breast and prostate cancer (40, 41). Because we and others have shown that osteoclasts are not involved in these early phases of bone marrow colonization (42–14), the newly identified prometastatic role of IL-1β might be exerted through either autocrine trophic stimulation of cancer cells, or a more complex paracrine recruitment of surrounding bone stromal cells other than osteoclasts. In the latter scenario, IL-1β would stimulate cells of the bone stroma and induce them to reciprocate with increased or *ex novo* production of trophic factors that would support the survival and growth of DTCs (44). In a recent study, Weinberg and colleagues have shown that IL-1β derived from carcinoma cells increases the expression of the COX-2 enzyme in MSCs of the tumor stroma and the consequent secretion of prostaglandin E_2 (PGE_2). The effect of PGE2 is exerted through a direct paracrine stimulation of the cancer cells and the autocrine induction of cytokine secretion from MSCs (19). Thus, we sought to ascertain whether a similar model could be applied to the prometastatic role of IL-1β revealed by our studies. To this end, we exposed human MSCs to media conditioned by PC3-ML cells and measured the effects on COX-2 expression after 48 hours. We concluded that the increase in COX-2 observed in MSCs was induced by the IL-1β secreted by PC3-ML cells, as the IL-1R antagonist Anakinra (45) was able to completely prevent it (Fig. 6). On the basis of this observation, further experiments are being

Published OnlineFirst March 27, 2013; DOI: 10.1158/0008-5472.CAN-12-3970

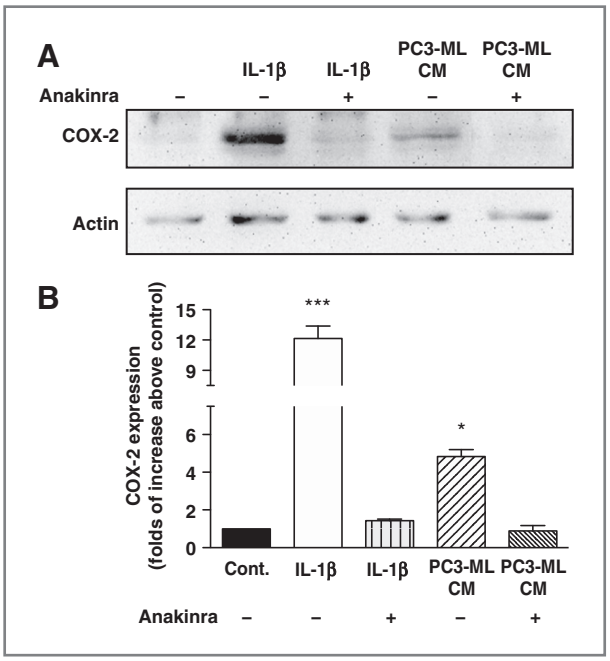

Figure 6. Overexpression of COX-2 induced by IL-1β secreted by bone-metastatic cancer cells. Human bone MSCs were exposed for 48 hours to a medium conditioned by PC3-ML cells and showed an evident increase in COX-2 expression, which was inhibited by pretreatment with the IL-1R inhibitor Anakinra (10 μg/mL). This effect was similar to that observed when MSCs were exposed directly to IL-1β (0.1 ng/mL; A). B, densitometry analysis of COX-2 expression from 3 different experiments showing similar results. *, $P < 0.05$; ***, $P < 0.001$.

conducted in our laboratory to conclusively establish the role of COX-2 and PGE_2 in the bone metastatic progression of prostate cancer cells.

Our study emphasizes the importance of early survival of DTCs mediated by IL-1β for successful lodging and initial colonization of the bone. These events are particularly relevant for the seeding of additional tumors by circulating tumor cells dislodged from preexisting lesions and commonly detected in the peripheral blood of patients with metastatic disease (46–48). Thus, disrupting the functional interactions between IL-1β and its receptors, most likely IL-1R, would substantially attenuate the progression of prostate cancer at the skeletal level and possibly reduce the secondary involvement of other organs.

Notably, therapeutics that target either IL-1β or IL-1R are currently available and prescribed for skeletal inflammatory conditions of non-neoplastic etiology such as rheumatoid arthritis (45, 49, 50). The evidence provided by our study should lead to the repositioning of these drugs in the clinic and rapidly translate into novel strategies for treating existing metastatic skeletal lesions as well as preventing ongoing seeding of additional lesions both in bone and visceral organs.

Disclosure of Potential Conflict of Interest

No potential conflicts of interest were disclosed.

Authors' Contributions

Conception and design: Q. Liu, K. Shahriari, A. Fatatis
Development of methodology: Q. Liu, M.R. Russell, K. Shahriari, F.U. Garcia
Acquisition of data (provided animals, acquired and managed patients, provided facilities, etc.): Q. Liu, M.R. Russell, K. Shahriari, F.U. Garcia
Analysis and interpretation of data (e.g., statistical analysis, biostatistics, computational analysis): Q. Liu, M.I. Lioni, F.U. Garcia, A. Fatatis
Writing, review, and/or revision of the manuscript: Q. Liu, K. Shahriari, D.L. Jernigan, M.I. Lioni, F.U. Garcia, A. Fatatis
Administrative, technical, or material support (i.e., reporting or organizing data, constructing databases): Q. Liu M.R. Russell, D.L. Jernigan, A. Fatatis
Study supervision: A. Fatatis

Acknowledgments

The authors thank Dr. Olimpia Meucci (Drexel University College of Medicine) for input and commentary and gratefully acknowledge the expertise and advice with the gene-expression analyses provided by Dr. Paolo Fortina (Dept. of Cancer Biology, Thomas Jefferson University and Kimmel Cancer Center, Philadelphia, PA), and the excellent technical assistance of Shankar Addya and Kathryn Scott (Cancer Genomic Microarray Facility, Kimmel Cancer Center, Philadelphia, PA).

Grant Support

This work was supported by the Prostate Cancer Program of the Department of Defense with the grant W81XWH-09-1-0724 (A. Fatatis).

The costs of publication of this article were defrayed in part by the payment of page charges. This article must therefore be hereby marked *advertisement* in accordance with 18 U.S.C. Section 1734 solely to indicate this fact.

Received October 17, 2012; revised March 19, 2013; accepted March 20, 2013; published OnlineFirst March 27, 2013.

References

1. Moul JW, Evans CP, Gomella LG, Roach M, Dreicer R. Traditional approaches to androgen deprivation therapy. Urology 2011;78:S485–93.
2. Kelly WK, Gomella LG. Androgen deprivation therapy and competing risks. JAMA 2011;306:2382–3.
3. Attard G, Reid AHM, Olmos D, de Bono JS. Antitumor activity with CYP17 blockade indicates that castration-resistant prostate cancer frequently remains hormone driven. Cancer Res 2009;69:4937–40.
4. Knudsen KE, Penning TM. Partners in crime: deregulation of AR activity and androgen synthesis in prostate cancer. Trends Endocrinol Metab 2010;21:315–24.
5. Hörnberg E, Ylitalo EB, Crnalic S, Antti H, Stattin P, Widmark A, et al. Expression of androgen receptor splice variants in prostate cancer bone metastases is associated with castration-resistance and short survival. Dent P editor. PLoS ONE 2011;6:e19059.
6. Debes JD, Tindall DJ. The role of androgens and the androgen receptor in prostate cancer. Cancer Lett 2002;187:1–7.
7. Yang JC, Ok J-H, Busby JE, Borowsky AD, Kung H-J, Evans CP. Aberrant activation of androgen receptor in a new neuropeptide-autocrine model of androgen-insensitive prostate cancer. Cancer Res 2009;69:151–60.
8. Beltran H, Rickman DS, Park K, Chae SS, Sboner A, MacDonald TY, et al. Molecular characterization of neuroendocrine prostate cancer and identification of new drug targets. Cancer Discov 2011;1:487–95.
9. Sun Y, Niu J, Huang J. Neuroendocrine differentiation in prostate cancer. Am J Transl Res 2009;1:148–62.
10. Jiborn T, Bjartell A, Abrahamsson PA. Neuroendocrine differentiation in prostatic carcinoma during hormonal treatment. Urology 1998;51:585–9.
11. Puccetti L, Supuran CT, Fasolo PP, Conti E, Sebastiani G, Lacquaniti S, et al. Skewing towards neuroendocrine phenotype in high grade or high stage androgen-responsive primary prostate cancer. Eur Urol 2005;48:215–21.

Published OnlineFirst March 27, 2013; DOI: 10.1158/0008-5472.CAN-12-3970

12. Cheville JC, Tindall D, Boelter C, Jenkins R, Lohse CM, Pankratz VS, et al. Metastatic prostate carcinoma to bone: clinical and pathologic features associated with cancer-specific survival. Cancer 2002;95: 1028–36.
13. Dolloff NG, Shulby SS, Nelson AV, Stearns ME, Johannes GJ, Thomas JD, et al. Bone-metastatic potential of human prostate cancer cells correlates with Akt/PKB activation by alpha platelet-derived growth factor receptor. Oncogene 2005;24:6848–54.
14. Russell MR, Jamieson WL, Dolloff NG, Fatatis A. The alpha-receptor for platelet-derived growth factor as a target for antibody-mediated inhibition of skeletal metastases from prostate cancer cells. Oncogene 2009;28:412–21.
15. Russell MR, Liu Q, Lei H, Kazlauskas A, Fatatis A. The alpha-receptor for platelet-derived growth factor confers bone-metastatic potential to prostate cancer cells by ligand- and dimerization-independent mechanisms. Cancer Res 2010;70:4195–203.
16. Wang M, Stearns ME. Isolation and characterization of PC-3 human prostatic tumor sublines which preferentially metastasize to select organs in S.C.I.D. mice. Differentiation 1991;48:115–25.
17. Masters JR. Human cancer cell lines: fact and fantasy. Nat Rev Mol Cell Biol 2000;1:233–6.
18. Jamieson WL, Shimizu S, D'Ambrosio JA, Meucci O, Fatatis A. CX3CR1 is expressed by prostate epithelial cells and androgens regulate the levels of CX3CL1/fractalkine in the bone marrow: potential role in prostate cancer bone tropism. Cancer Res 2008;68:1715–22.
19. Li H-J, Reinhardt F, Herschman HR, Weinberg RA. Cancer-stimulated mesenchymal stem cells create a carcinoma stem cell niche via prostaglandin E2 signaling. Cancer Discov 2012;2:840–55.
20. Irizarry RA, Hobbs B, Collin F, Beazer-Barclay YD, Antonellis KJ, Scherf U, et al. Exploration, normalization, and summaries of high density oligonucleotide array probe level data. Biostatistics 2003;4:249–64.
21. Kaighn ME, Narayan KS, Ohnuki Y, Lechner JF, Jones LW. Establishment and characterization of a human prostatic carcinoma cell line (PC-3). Invest Urol 1979;17:16–23.
22. Tai S, Sun Y, Squires JM, Zhang H, Oh WK, Liang C-Z, et al. PC3 is a cell line characteristic of prostatic small cell carcinoma. Prostate 2011;71:1668–79.
23. Russell MR, Liu Q, Fatatis A. Targeting the {alpha} receptor for platelet-derived growth factor as a primary or combination therapy in a preclinical model of prostate cancer skeletal metastasis. Clin Cancer Res 2010;16:5002–10.
24. Mickey DD, Stone KR, Wunderli H, Mickey GH, Vollmer RT, Paulson DF. Heterotransplantation of a human prostatic adenocarcinoma cell line in nude mice. Cancer Res 1977;37:4049–58.
25. Stone KR, Mickey DD, Wunderli H, Mickey GH, Paulson DF. Isolation of a human prostate carcinoma cell line (DU 145). Int J Cancer 1978;21:274–81.
26. Bastian PJ, Gonzalgo ML, Aronson WJ, Terris MK, Kane CJ, Amling CL, et al. Clinical and pathologic outcome after radical prostatectomy for prostate cancer patients with a preoperative Gleason sum of 8 to 10. Cancer 2006;107:1265–72.
27. Yigitbasi O, Ozturk U, Goktug HNG, Gucuk A, Bakirtas H. Prognostic factors in metastatic prostate cancer. Urol Oncol 2011;29:162–5.
28. Abdul M, Hoosein N. Differences in the expression and effects of interleukin-1 and -2 on androgen-sensitive and -insensitive human prostate cancer cell lines. Cancer Lett 2000;149:37–42.
29. Culig Z, Klocker H, Bartsch G, Hobisch A. Androgen receptors in prostate cancer. Endocr Relat Cancer 2002;9:155–70.
30. Vashchenko N, Abrahamsson P-A. Neuroendocrine differentiation in prostate cancer: implications for new treatment modalities. Eur Urol 2005;47:147–55.
31. Yin J, Pollock C, Tracy K, Chock M, Martin P, Oberst M, et al. Activation of the RalGEF/Ral pathway promotes prostate cancer metastasis to bone. Mol Cell Biol 2007;27:7538–50.
32. Hoosein NM. Neuroendocrine and immune mediators in prostate cancer progression. Front Biosci 1998;3:D1274–9.
33. Leiblich A, Cross SS, Catto JWF, Pesce G, Hamdy FC, Rehman I. Human prostate cancer cells express neuroendocrine cell markers PGP 9.5 and chromogranin A. Prostate 2007;67:1761–9.
34. Miyoshi Y, Uemura H, Kitami K, Satomi Y, Kubota Y, Hosaka M. Neuroendocrine differentiated small cell carcinoma presenting as recurrent prostate cancer after androgen deprivation therapy. BJU Int 2001;88:982–3.
35. Frigo DE, McDonnell DP. Differential effects of prostate cancer therapeutics on neuroendocrine transdifferentiation. Mol Cancer Ther 2008;7:659–69.
36. Huss WJ, Gray DR, Tavakoli K, Marmillion ME, Durham LE, Johnson MA, et al. Origin of androgen-insensitive poorly differentiated tumors in the transgenic adenocarcinoma of mouse prostate model. Neoplasia 2007;9:938–50.
37. Shibue T, Weinberg RA. Metastatic colonization: settlement, adaptation and propagation of tumor cells in a foreign tissue environment. Semin Cancer Biol 2011;21:99–106.
38. Weilbaecher KN, Guise TA, Mccauley LK. Cancer to bone: a fatal attraction. Nat Rev Cancer 2011;11:411–25.
39. Evans DB, Bunning RA, Russell RG. The effects of recombinant human interleukin-1 beta on cellular proliferation and the production of prostaglandin E2, plasminogen activator, osteocalcin and alkaline phosphatase by osteoblast-like cells derived from human bone. Biochem Biophys Res Commun 1990;166:208–16.
40. Sturge J, Caley MP, Waxman J. Bone metastasis in prostate cancer: emerging therapeutic strategies. Nat Rev Clin Oncol 2011;8:357–68.
41. Higano CS. New treatment options for patients with metastatic castration-resistant prostate cancer. Cancer Treat Rev 2012;38:340–5.
42. Vukmirovic-Popovic S, Colterjohn N, Lhoták S, Duivenvoorden WCM, Orr FW, Singh G. Morphological, histomorphometric, and microstructural alterations in human bone metastasis from breast carcinoma. Bone 2002;31:529–35.
43. Lee Y, Schwarz E, Davies M, Jo M, Gates J, Wu J, et al. Differences in the cytokine profiles associated with prostate cancer cell induced osteoblastic and osteolytic lesions in bone. J Orthop Res 2006;21: 62–72.
44. Schulze J, Weber K, Baranowsky A, Streichert T, Lange T, Spiro AS, et al. p65-Dependent production of interleukin-1β by osteolytic prostate cancer cells causes an induction of chemokine expression in osteoblasts. Cancer Lett 2012;317:106–13.
45. Dinarello CA, Simon A, van der Meer JWM. Treating inflammation by blocking interleukin-1 in a broad spectrum of diseases. Nat Rev Drug Discov 2012;11:633–52.
46. Kim M-Y, Oskarsson T, Acharyya S, Nguyen DX, Zhang XH-F, Norton L, et al. Tumor self-seeding by circulating cancer cells. Cell 2009;139:1315–26.
47. Lin H, Balic M, Zheng S, Datar R, Cote RJ. Disseminated and circulating tumor cells: Role in effective cancer management. Crit Rev Oncol Hematol 2011;77:1–11.
48. Powell AA, Talasaz AH, Zhang H, Coram MA, Reddy A, Deng G, et al. Single cell profiling of circulating tumor cells: transcriptional heterogeneity and diversity from breast cancer cell lines. Chin W-C editor. PLoS ONE 2012;7:e33788.
49. Alten R, Gram H, Joosten LA, van den Berg WB, Sieper J, Wassenberg S, et al. The human anti-IL-1 beta monoclonal antibody ACZ885 is effective in joint inflammation models in mice and in a proof-of-concept study in patients with rheumatoid arthritis. Arthritis Res Ther 2008;10: R67.
50. Cardiel MH, Tak PP, Bensen W, Burch FX, Forejtova S, Badurski JE, et al. A phase 2 randomized, double-blind study of AMG 108, a fully human monoclonal antibody to IL-1R, in patients with rheumatoid arthritis. Arthritis Res Ther 2010;12:R192.
51. Taylor BS, Schultz N, Hieronymus H, Gopalan A, Xiao Y, Carver BS, et al. Integrative genomic profiling of human prostate cancer. Cancer Cell 2010;18:11–22.
52. Varambally S, Yu J, Laxman B, Rhodes DR, Mehra R, Tomlins SA, et al. Integrative genomic and proteomic analysis of prostate cancer reveals signatures of metastatic progression. Cancer Cell 2005;8:393–406.
53. Yu YP, Landsittel D, Jing L, Nelson J, Ren B, Liu L, et al. Gene expression alterations in prostate cancer predicting tumor aggression and preceding development of malignancy. J Clin Oncol 2004;22: 2790–9.
54. Singh D, Febbo PG, Ross K, Jackson DG, Manola J, Ladd C, et al. Gene expression correlates of clinical prostate cancer behavior. Cancer Cell 2002;1:203–9.

Supplementary Information

Interleukin-1β promotes skeletal colonization and progression of metastatic prostate cancer cells with neuroendocrine features.

Qingxin Liu, Mike Russell, Kristina Shahriari, Danielle Jernigan, Mercedes I. Lioni, Fernando U. Garcia and Alessandro Fatatis

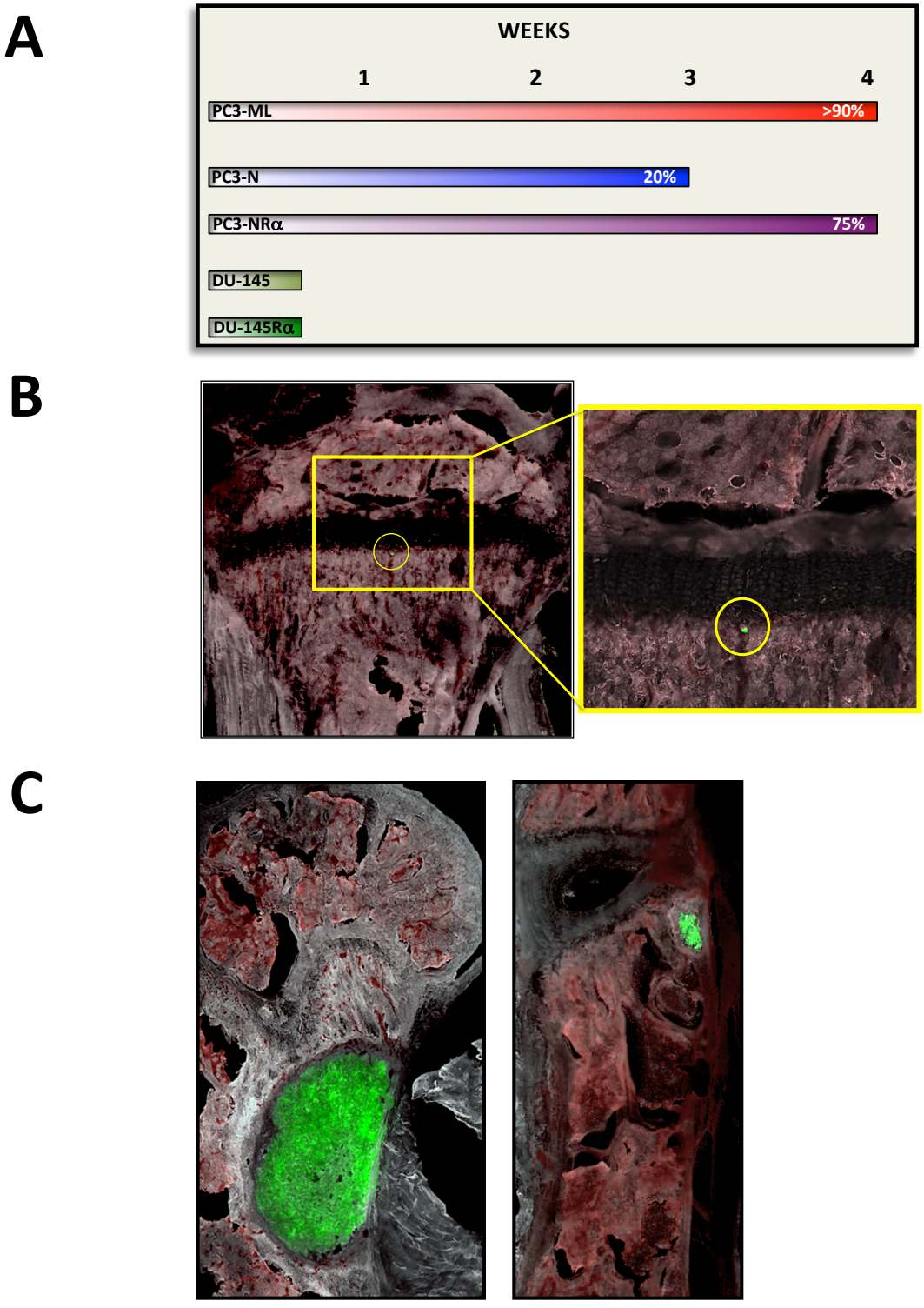

Supplementary Figure 1. Metastatic progression of different human prostate cancer cells in the skeleton of animal model. After being inoculated in the arterial circulation, PC3-ML and PC3-N(Rα) produce metastatic bone lesions in 90% and 75% of mice, respectively. PC3-N cells show weak metastatic potential and generate bone lesions in only 20% of animals inspected three weeks post-inoculation. No lesions were detected in mice inoculated with PC3-N cells and inspected four weeks later, which suggests that the small number of lesions detected at three weeks eventually regress. DU-145 and DU-145(Rα) cells never progress past the stage of DTCs and are detected only within three days post-inoculation (**a**); DU-145 as DTCs in the tibia of an inoculated animal (**b**); large metastatic tumors produced by PC3-ML cells in the femur (left) and spine (right) of a mouse inoculated four weeks earlier (**c**).

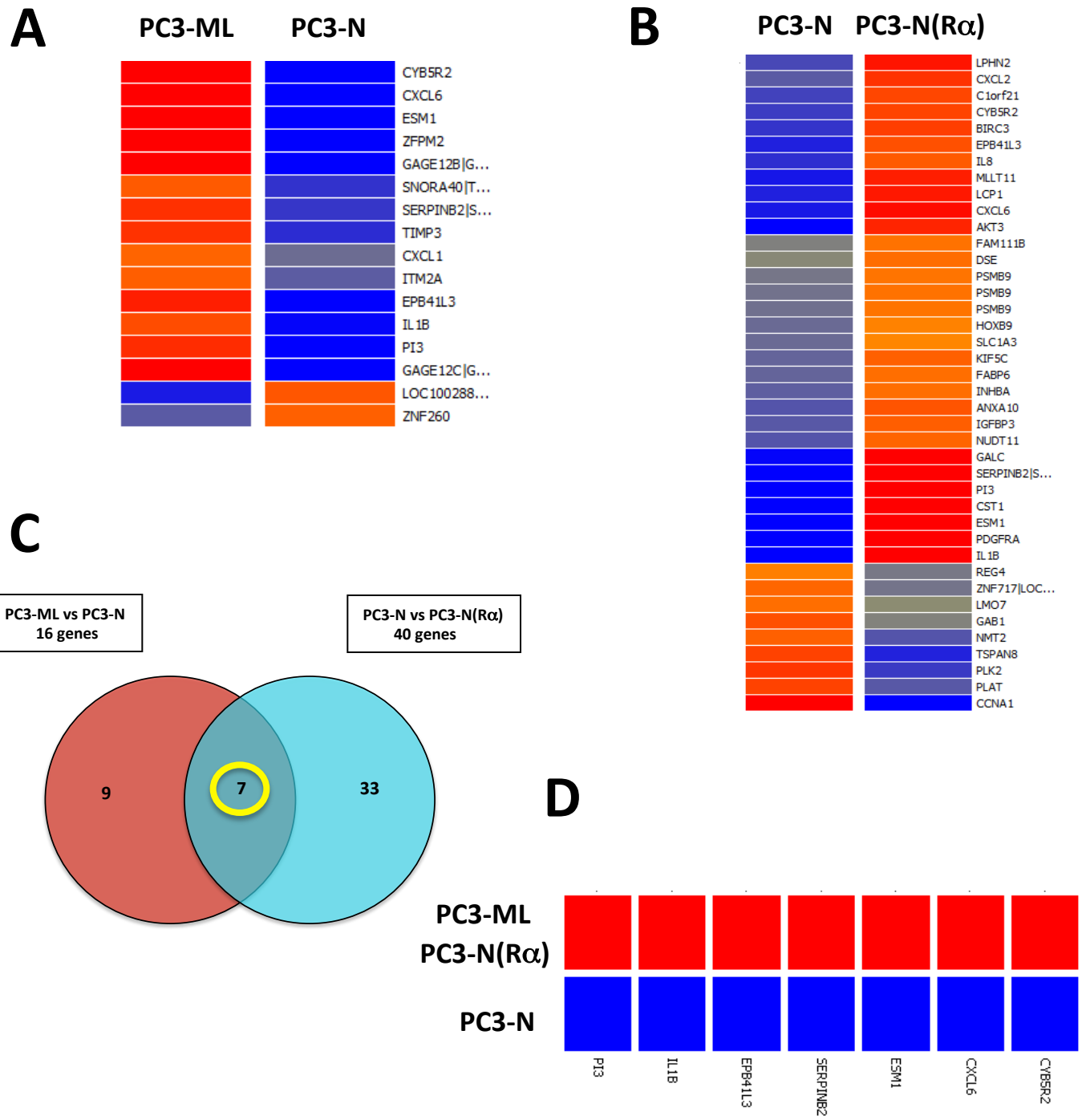

Supplementary Figure 2. Identification of pro-metastatic genes regulated by PDGFRα in PC3 cells. PC3-ML cells (high PDGFRα) and PC3-N cells (low PDFGRα) showed 16 differentially regulated genes (**a**); the exogenous expression of PDGFRα in PC3-N cells regulated 40 genes (**b**); Venn diagram showing 7 genes that were found overlapping between the 16 and 40 genes identified above (**c**); the newly-identified genes directly correlate with high levels of PDGFRα expression and the bone-metastatic progression of PC3 cells (**d**).

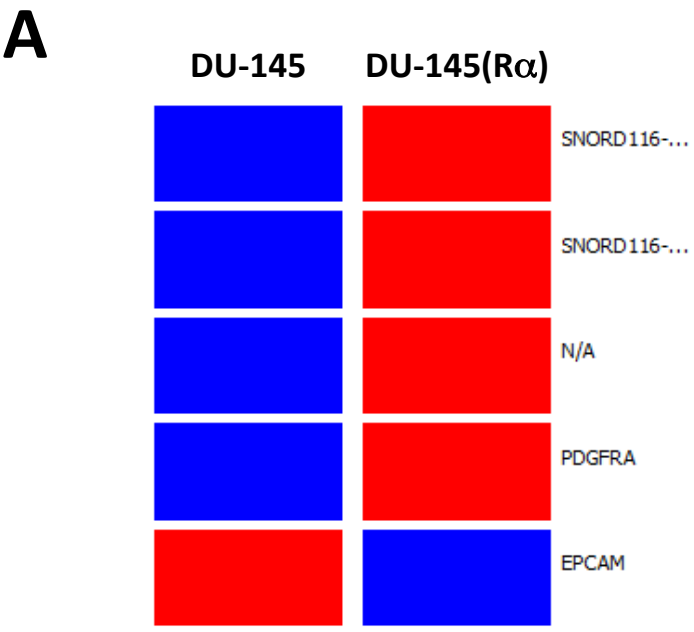

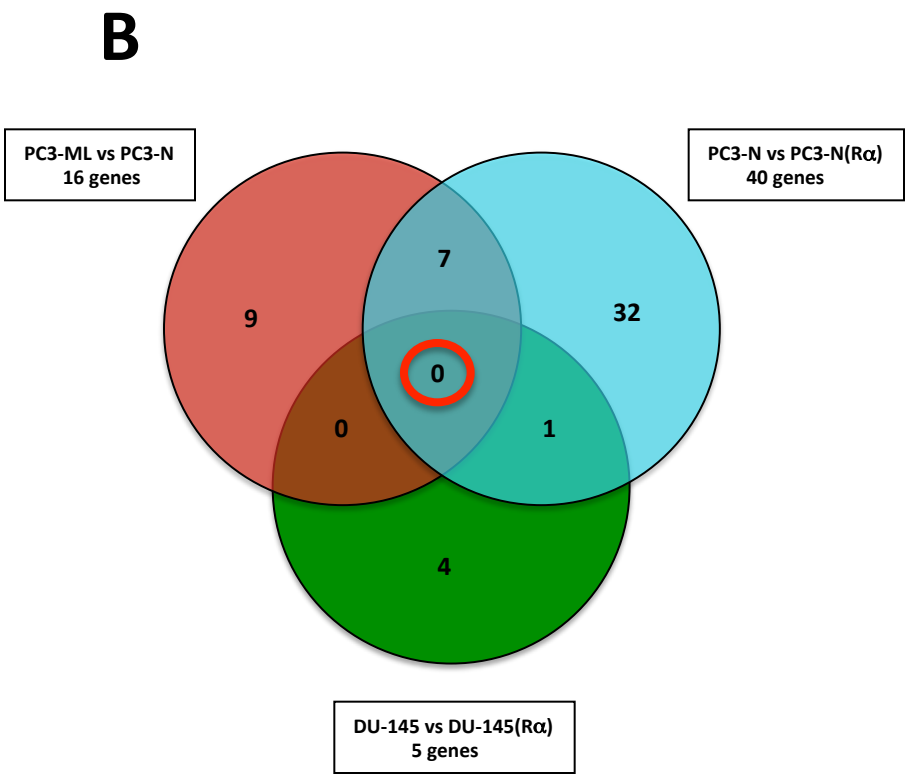

Supplementary Figure 3. Genes regulated by PDGFRα in DU-145 cells, which did not acquire bone-metastatic behavior upon exogenous expression of this receptor.
Five genes were regulated by PDGFRα in DU-145 cells (**a**); none of these genes showed overlap with the seven genes regulated by PDGFRα in PC3 cells (**b**).

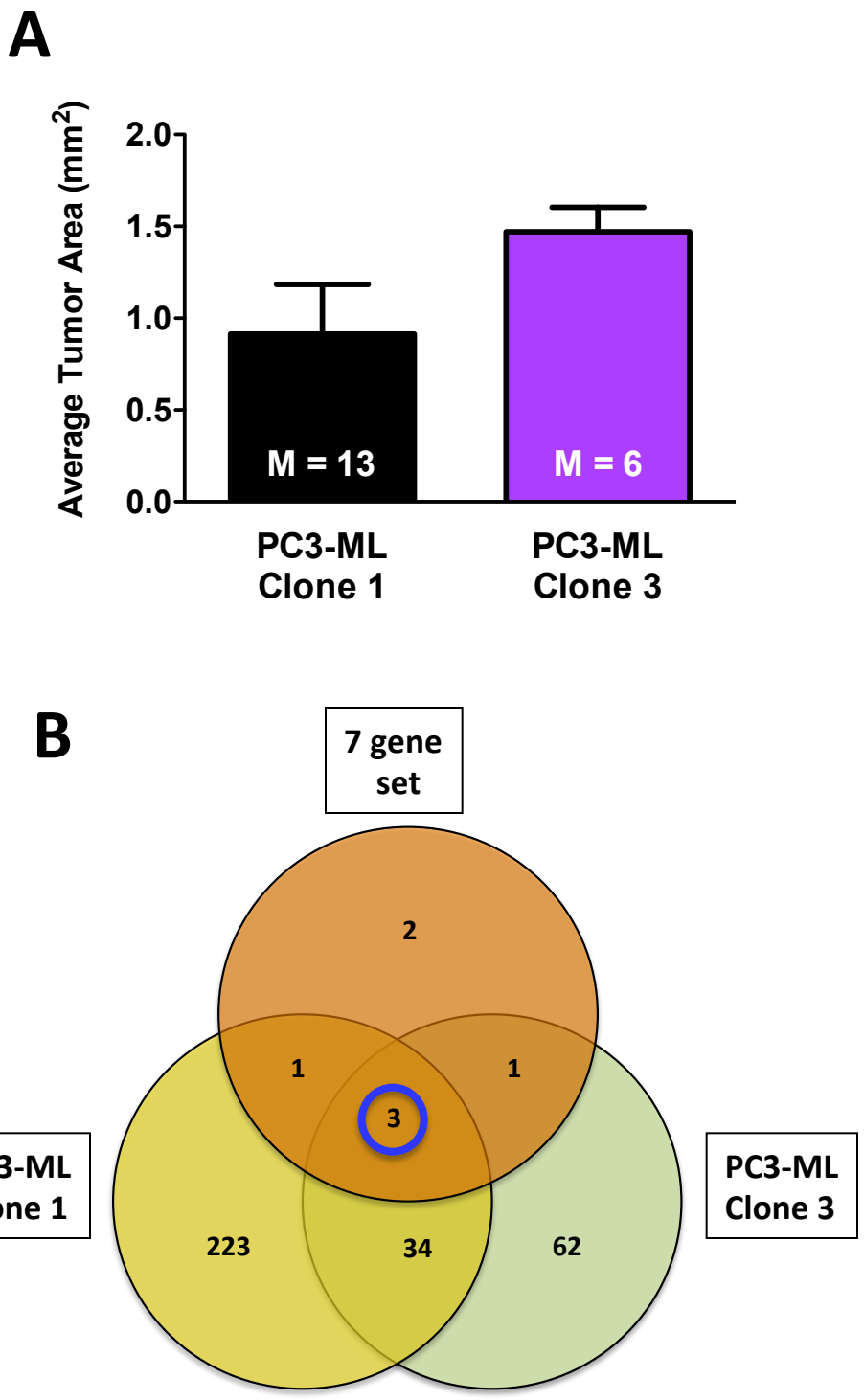

Supplementary Figure 4. Two single-cell progenies of PC3-ML cells with high bone-metastatic potential. Clone 1 and Clone 3 were inoculated in five mice each and generated large skeletal lesions in all animals (**a**); Venn diagram showing overlap of genes differentially regulated between Clone 1 and Clone 3 and their overlapping with the 7-gene set identified in figure S3. Three genes were strongly associated with metastatic behavior of prostate cancer cells in animal models (**b**).

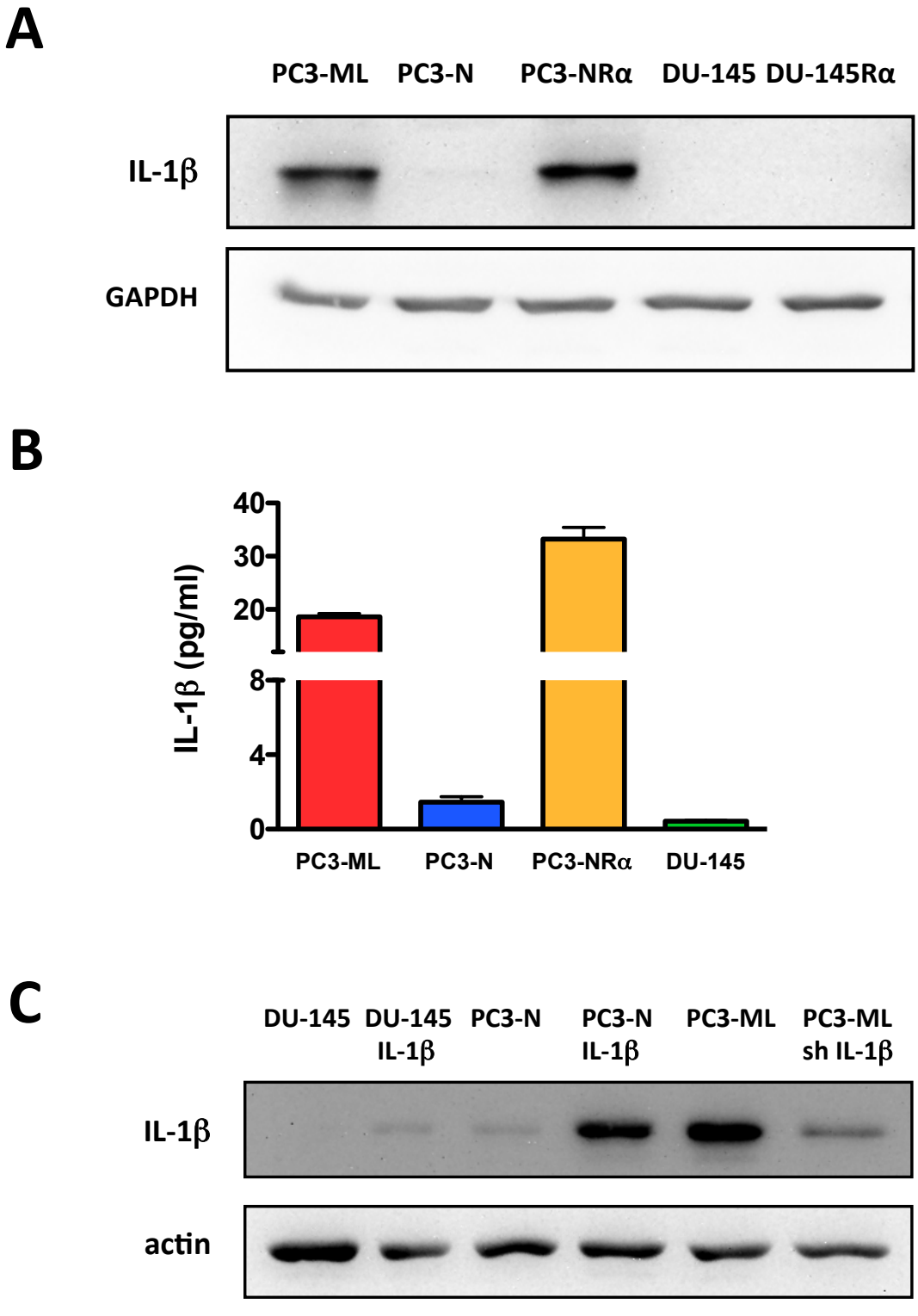

Supplementary Figure 5. Analysis of IL-1β expression and secretion from prostate cancer cells. PC3-ML cells showed higher levels of IL-1β expression as compared to PC3-N cells and the exogenous over-expression of PDGFRα up-regulated IL-1β expression in PC3-N cells. In contrast, PDGFRα did not increase IL-1β expression in DU-145 cells (**a**); the levels of IL-1β secreted by different cell types and measured by ELISA confirmed the Western Blotting results. All together these data provide full validation of the gene expression microarray analyses (**b**); over-expression or silencing of IL-1β in different cell types that were tested in our animal model for their respective metastatic behavior (**c**).

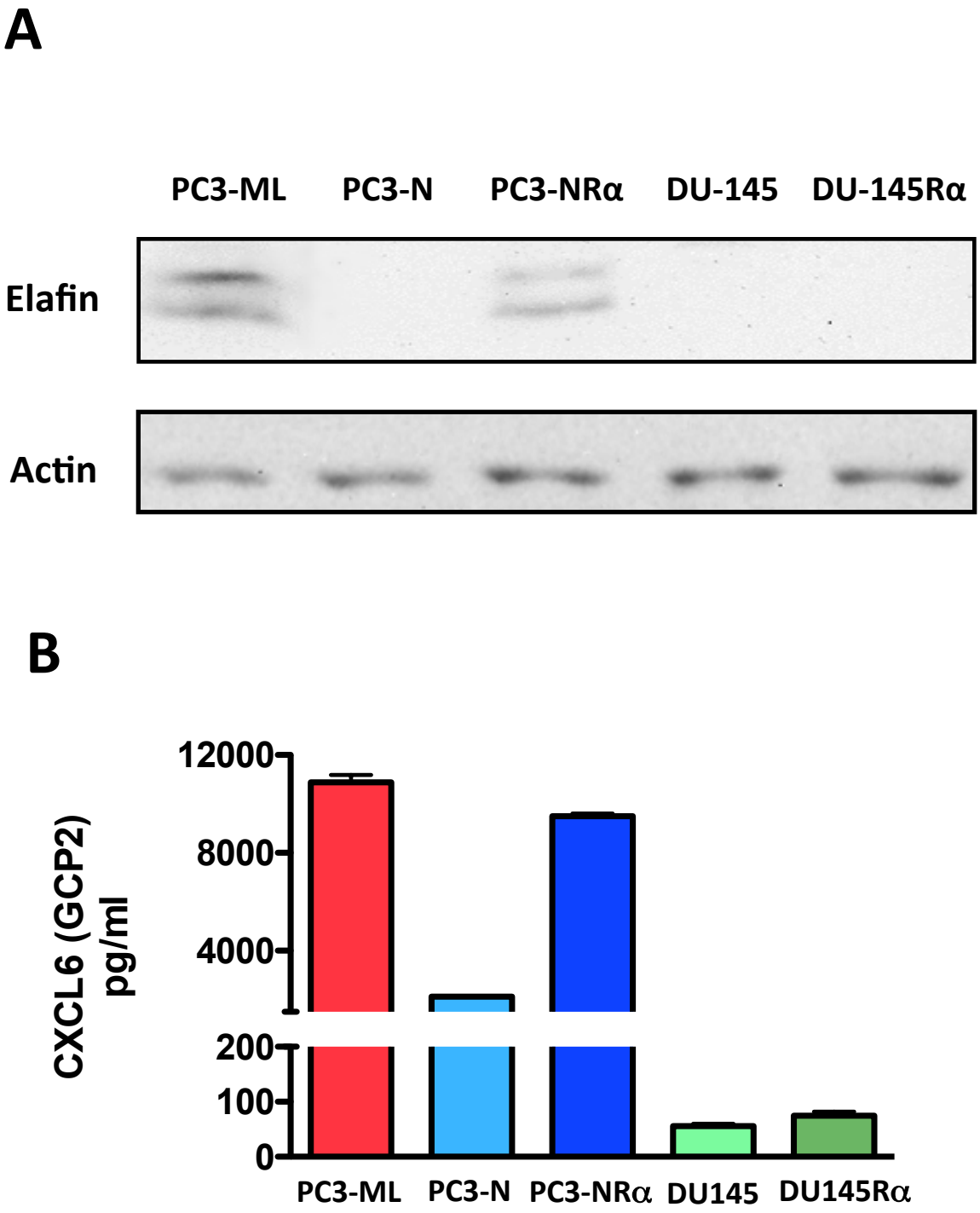

Supplementary Figure 6. PDGFRα regulates Elafin and CXCL6 expression in prostate cancer cells. PC3-ML cells express higher levels of Elafin as compared to PC3-N cells and the over-expression of PDGFRα upregulates this protein in PC3-N cells but not in DU-145 cells (**a**); a similar pattern of PDGFRα regulation can be observed for CXCL6 when measured as secreted protein in the same cells (**b**). Both sets of data are in full agreement with the results of the microarray analysis.

GLEASON	Intensity of IL-1β			TOTAL
	0/1+	2+	3+	
< 7	38	35	8	81
≥ 7	22	73	51	146

Supplementary Table 1. Contingency table of TMA data showing that prostate tumors with Gleason scores (≥7) expressed higher levels of the IL-1β protein as compared to tumors with lower Gleason scores (<7) (**E**). Chi-square = 33.08 and $p<0.0001$